

Bound states of charges on top of graphene in magnetic field

Sergey Slizovskiy*

*Department of Physics, Loughborough University,
Loughborough LE11 3TU, UK and
NRC “Kurchatov Institute” PNPI, Russia*

We show theoretically that in the external magnetic field like charges on top of graphene monolayer may be mutually attracted to form macro-molecules. For this to happen graphene needs to be in Quantum Hall plateau state with chemical potential between the Landau levels. Graphene electron(s) gets localized in the middle between charges and provides overscreening of Coulomb repulsion between the charges. The size of the resulting macro-molecules is of the order of the magnetic length (~ 10 nm for magnetic field 10 T). All the possible stable macro-molecules that unit charges can form on graphene in magnetic field are classified. The binding survives significant temperatures, exceeding mobility barriers for many ionically bond impurities.

Tuning the doping of graphene or the magnetic field, the binding of impurities can be turned on and off and the macro-molecule size may be tuned. This opens the perspective to nanoscopic manipulation of ions on graphene by using magnetic field and gating.

PACS numbers: 75.70.Ak , 73.22.Pr, 12.20.Ds

I. INTRODUCTION

More than ten years since discovery of graphene¹, the first genuinely two-dimensional material, are marked with huge body of research. It's applications range from cancer-drug delivery^{2,3} to novel electronic devices. Still, many of proposed uses of graphene depend crucially on it's interface interactions with other compounds and impurities. Typically, molecular dynamics and DFT methods⁴⁻⁹ are used to model the interaction of graphene with substrate and impurities. It was shown that there are two types of impurity bonding to graphene⁴: covalently bond impurities (e.g. H, CH₃, F, OH, O) and ionically bond impurities (e.g. Na, K, Cs, Cl, Br, I). Covalently bond impurities act similar to defects in graphene structure and typically have large mobility barriers, while ionically bond impurities have low mobility barriers (typically lower than room temperature) and act as mobile electric charges put on top of graphene^{4,10,11}.

Interaction between impurities has attracted significant experimental and theoretical interest. It was shown¹² that short-range covalently bond impurities tend to form bound clusters due to a fermionic Casimir effect with binding energy comparable to room temperature scale at distances below 2 nm. On the other hand, this effect cannot compete with Coulomb repulsion of like charges if the impurities are charged, as is the case for ionically bond impurities.

Graphene is known to be exceptionally susceptible to magnetic field with divergent diamagnetic susceptibility at the Dirac point and strong non-linear effects in magnetization^{13,14}. Magnetic field creates large energy gaps near the Dirac point that reduce intrinsic screening and help to localize electrons in the external potentials. In this work we discuss the interaction between charged impurities near the sur-

face of graphene in the strong magnetic field and show that in some cases the binding due to electrons in graphene can compete with Coulomb repulsion and stable nano-molecules may form. The motivation for this work comes not only from ionically bond impurities mentioned above: Epitaxial graphene on Si-terminated SiC¹⁵⁻¹⁸ has an important feature of positively-charged donors appearing dynamically in the “dead” carbon layer just below graphene¹⁹⁻²¹. This happens due the dominant effect of quantum capacitance²² and due to strong changes in the density of states near the Dirac point under the influence of magnetic field^{19,23}. The process looks as the appearance of localized holes in the insulating “dead” layer due to electrons transferred to graphene. Consequently, the charge transfer might dynamically create extra localized states and extra electrons to keep the system in a robust $\nu \approx 2$ quantum Hall plateau state. Since the charge transfer is reversible, the holes below graphene can be considered on the same footing as dynamical charged impurities.

For definiteness, we consider positively charged ions below, but exactly the same description applies to the negative ions if one makes a particle-hole transformation and reverts the sign of chemical potential.

Without magnetic field, graphene will produce non-linear screening of external charges^{24,25}. When magnetic field is applied, the ordinary screening is significantly suppressed^{26,27} and electrons become localized. We show that when several charged impurities are at the distance of the order of magnetic length $l_B = \sqrt{\hbar/(eB)}$, they can form stable molecules bound by the electrons in graphene. Depending on its local chemical potential, graphene may bind either positive ions, or negative, or produce no significant binding at all, the results are summarized in Table I and Fig.3. The described

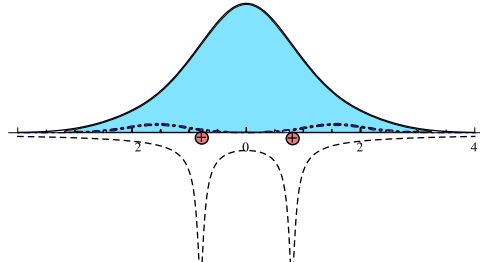


FIG. 1. Illustration of A and B sublattice wavefunctions $|\psi_A|^2$, $|\psi_B|^2$ for the lowest-energy sublevel of 0-th LL; and Coulomb potential of two charges (dashed).

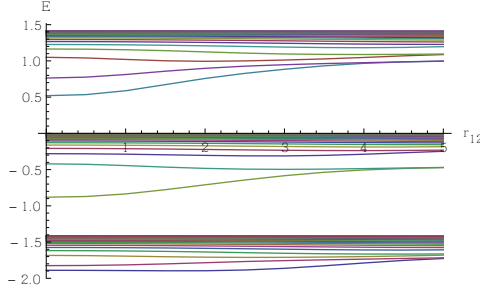


FIG. 2. Illustration of energy sub-levels for three Landau levels as a function of distance between two positively charged Coulomb centers. Here $\alpha = 0.4$ and $d = 0.05$.

effect may be called either as *over-screening of Coulomb repulsion of impurities* or as *long range covalent bonding of charged impurities*. Graphene in magnetic field hosts the electron hybridization cloud that can lead to attraction exceeding the Coulomb repulsion of same-charge ions, see Fig.1. Similarly to the signatures of Quantum Hall Effect (QHE)²⁸, we show that the effect may survive the room temperature for magnetic fields of order 10 T.

TABLE I. Stable states of N positively charged ions bound by n electrons at $\alpha = 0.4$, $d = 0.05l_B$; for negatively-charged ions one has to replace $\mu \rightarrow -\mu$

№	μ_{\min}	N ions	n electrons	$r_{ij}(l_B)$	E
1	-0.93	3 triangle	2 symm.	1.5	-1.06
2	-0.75	2	1	1.7	-0.52
3	-0.63	2	2 symm.	1.3	-0.96
4	-0.45	1	1	-	-0.45
5	-0.28	1	2 symm.	-	-0.56
6	0.51	3 triangle	2 symm.	1.4	1.88
7	0.67	2	1	1.5	0.94
8	0.82	2	2 symm.	1.2	1.98
9	1.02	1	1	-	1.02
10	1.19	1	2 anti-symm.	-	2.38

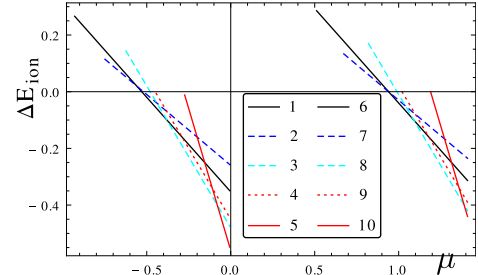


FIG. 3. Zero-temperature phase diagram for dilute mobile charged impurities. Phase with lowest ΔE_{ion} is favored. Legend corresponds to Table I.

II. GRAPHENE WITH CHARGED IMPURITIES IN MAGNETIC FIELD

It is well-known that the one-particle energy levels of an ideal graphene in magnetic field B are given by degenerate Landau levels^{1,29–31}:

$$E_n = \text{sign}(n)E_B \sqrt{2|n|}, \quad n \in \mathbb{Z} \quad (1)$$

where $v_F \approx 10^6 \text{ m/s}$,

$$l_B = \sqrt{\hbar/(eB)} \approx 26/\sqrt{B/(\text{Tesla})} \text{ nm} \quad (2)$$

$$E_B \equiv \frac{\hbar v_F}{l_B} \approx 26\sqrt{B/(\text{Tesla})} \text{ meV}. \quad (3)$$

Each Landau level (LL) is degenerate with density $4\frac{e}{2\pi\hbar}B$ per unit area. Working with finite area, it is convenient to use the basis of Landau wave-functions in polar coordinates. Defining an oscillator radial eigenfunction:

$$g_{n,m}(r) = e^{-\frac{r^2}{4}} r^{|m|} \sqrt{\frac{2^{-|m|}(|m|+n)!}{2\pi n!(|m|!)^2}} {}_1F_1\left(-n; |m|+1; \frac{r^2}{2}\right)$$

we have for the wave-functions ($m < n$, $n > m$):

$$\psi_{0,m}(r, \phi) = \begin{pmatrix} 0 \\ e^{im\phi} g_{0,m}(r) \end{pmatrix}, \quad m \leq 0 \quad (4)$$

$$\psi_{\pm n,m}(r, \phi) = \frac{e^{im\phi}}{\sqrt{2}} \begin{pmatrix} \mp e^{-i\phi} g_{n-\frac{m-1+|m|-1}{2}, m-1}(r) \\ i g_{n-\frac{m+|m|}{2}, m}(r) \end{pmatrix}$$

When the Coulomb impurity potential is present, the orbital (index m) degeneracy of Landau levels is lifted²⁷. This has been calculated^{27,32,33} and demonstrated experimentally²⁷ for one Coulomb impurity. Below we consider several impurities.

Consider a superposition of Coulomb potentials of the form

$$U(\vec{r}) = -\frac{e^2}{4\pi\epsilon_0\epsilon} \sum_i \frac{1}{\sqrt{(\vec{r} - \vec{r}_i)^2 + d^2}} \quad (5)$$

Here the parameter d is a vertical displacement of impurity from the graphene sheet, but it can also be

used to model a finite localization length of impurity wave-function³⁴. Assuming the charged impurity wave-function to be reasonably smooth on the lattice scale, we use the low-energy effective mass approximation and neglect the inter-valley scattering. This approximation is reasonable since the main effect we discuss comes from the full range of Coulomb potential and not from short-range scattering as in Ref. 12. This is further confirmed by the weak dependence of binding force on the effective range of impurity wave function, see Fig.4. The equations for electron energy levels in graphene in the magnetic field B and any Coulomb potentials can be rewritten³² in units of magnetic length l_B , magnetic energy E_B and dimensionless coupling

$$\alpha = e^2 / (4\pi\epsilon_0\hbar v_F\epsilon_{\text{eff}}) = 2.19/\epsilon_{\text{eff}} \quad (6)$$

with the effective dielectric constant $\epsilon_{\text{eff}} = (\epsilon_1 + \epsilon_2)/2$ coming from substrates on both sides of graphene and from graphene by itself. For example, $\alpha \approx 1$ on SiO_2 substrate²⁷ and $\alpha \approx 0.4$ on SiC . In dimensionless units the equation to solve is³²

$$[\sigma_1(i\partial_x - y) - i\sigma_2\partial_y]\Psi = \left(E - \sum_{i=1}^N \frac{\alpha}{\sqrt{(\vec{r} - \vec{r}_i)^2 + d^2}} \right) \Psi$$

For performing the computations we evaluate the matrix elements of the impurity potential in the basis (4) truncated to several Landau levels (of the order of 10) and orbital states (of order of 30) and then do an exact diagonalization. The truncation of orbital states we use corresponds to a circular box truncation of space and to avoid unphysical boundary contributions we had to smoothly cut-off the Coulomb potential at large distances (of order of $4l_B$). As a result, for inter-ion distances up to $2l_B$, the precision is better than 1% while for larger distances the error may get higher.

The Landau levels that are completely filled do not contribute significantly to the energy of ions as a function of their separation, this has been verified numerically and is seen analytically in the leading order of perturbation theory in the potential:

$$E(r_{12}) \sim \sum_m \langle \psi_{n,m}^{(0)} | V(\vec{r} - \vec{r}_1) + V(\vec{r} - \vec{r}_2) | \psi_{n,m}^{(0)} \rangle = 2 \sum_m \langle \psi_{n,m}^{(0)} | V(\vec{r}) | \psi_{n,m}^{(0)} \rangle = \text{const} \quad (7)$$

where we used that the full degenerate set of wave-functions, corresponding to a given Landau level (enumerated by m) maps to itself under translations (up to a unitary transformation), and so the above sum is independent of the impurity positions.

The situation changes drastically if only one or several lowest Landau sub-levels are filled with electrons. This happens when graphene is in Quantum Hall plateau state corresponding to the chemical potential being in between the unperturbed LLs.

Let us start with two positive charges $N = 2$. The single-particle energy levels of electrons in graphene are presented on Fig.2. When the distance between the two ions is of the order of magnetic length l_B , the lowest energy electron wave-function is *centered in the middle between the ions* and plays the role of hybridization cloud that binds them, Fig. 1. When only this lowest-energy state is filled, the strong dependence of energy on the distance r_{12} between ions appears, Fig. 2, creating the attractive force, Fig. 4. If the distance between charges exceeds roughly $3l_B$, the lowest energy electron wave-function becomes centered near each of the individual charges and its energy depends on r_{12} as $E \sim -1/r_{12}$ due to the trivial tail of Coulomb potential. This means that each charge becomes individually screened and only a weak dipole-dipole attraction between them is expected.

In the leading order of perturbation theory, the binding force is proportional to α . Notably, the mutual Coulomb repulsion of ions is also proportional to α :

$$E_{\text{Coulomb}} = \frac{\alpha}{r_{12}} \quad (8)$$

Thus, in the leading approximation the distance where the attraction would balance the repulsion is independent of α . We stress here that when expressed in magnetic length and energy units, there are essentially no free parameters in the problem and the Coulomb repulsion of ions is of the same order of magnitude as hybridization attraction.³⁵ It is a priori not at all clear if stable bound states of ions can form. Moreover, strong bound states form only when the chemical potential μ is near the 0-th and 1-st Landau levels. When μ is near the other Landau levels (see Fig. 2), the r_{12} dependence of electron energy is substantially weaker leading to weaker binding of ions. The main problem with bound states in the higher plateau states is that they will not survive graphene rippling and temperature, thus we concentrate on the most robust $\nu \approx \pm 2$ plateau states below.

Let us first study the dependence on the coupling constant α , see Fig. 4b. We observe that the 0-th LL is almost protected from non-linearity, while a significant non-linearity appears in the higher LL already at $\alpha \sim 0.1$. The 1-st and -1-st levels must have the same energies in the leading order of perturbation theory as their wave-functions differ only by a relative sign of sublattice components, but we see that these levels split already from $\alpha \sim 0.1$. This could be expected due to large Coulomb field near an individual impurity. Similar asymmetry is present in the results of ref.27. The dependence on the distance d of the ion from graphene (or, on the localization length of charge wave-function) is weak when this distance is much less than magnetic length, see Fig.4c.

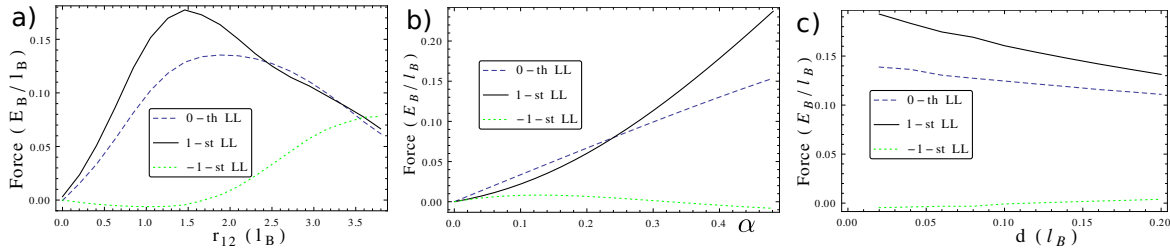


FIG. 4. Binding force of two ions bound by one electron: a) as a function of inter-ion distance r_{12} for $\alpha = 0.4$ and $d = 0.05l_B$; b) as a function of coupling α for $d = 0.05l_B$ and $r_{12} = 1.5l_B$; c) as a function of d (distance of ions from the graphene sheet) for $\alpha = 0.4$, $r_{12} = 1.5l_B$

Below we present a particular example of $\alpha = 0.4$, $d = 0.05l_B$, the results are universal for 0-th LL, while for the 1-st LL the binding is seen to grow a bit faster than linear in α .

The results for two positive ions bound by one electron are presented on Fig.5a. We observe an absolute minimum in the energy at a distance $r_{12\min} \approx 1.5l_B$ near the 1-st LL or $1.7l_B$ near the 0-th LL.

If the chemical potential decreases below a critical value, determined as the energy per electron in the bound state, see Table I, there will be no bound states for positive ions, but, at some point, we start getting bound states for negatively charged impurities bound by holes. The calculations and results for negatively charged impurities are exactly the same and obtained by going to hole picture.

Analogous calculation shows that the configurations with three symmetrically positioned impurities bound by one electron is unstable: despite an appearance of local energy minimum, the configuration would gain energy if deformed to a bound pair with the third ion repelled to infinity.

Now consider multi-electron bound states. The two-electron bound state can be in a symmetric or antisymmetric orbital state. In a conventional molecule this would correspond to spin singlet and triplet respectively, but in graphene one has an additional valley degeneracy^{13,36} and the full $SU(4)$ symmetry is approximately respected (neglecting the Zeeman splitting). Group theory tells us that $\mathbf{4} \otimes \mathbf{4} = \mathbf{10} \oplus \mathbf{6}$ in spin-valley space, so, there are 10 possibilities to form antisymmetric orbital state and 6 for symmetric one.

To find a reasonable approximation to the energy, we use the variational Hartree-Fock method with the basis formed by Slater determinants of low-energy 1-particle eigenstates found above.

Looking at Fig.2 we note that near the 1-st LL the two lowest energy levels grow with r_{12} thus can potentially bind the ions and can participate in antisymmetric orbital wave-function. For the 0-th LL only the lowest level binds the ions while electrons in the higher levels do not tend to hybridize, thus the orbital wave-function can only be symmetric for a stable ion-binding.

Consider two electrons in the field of a single ion. For $\alpha = 0.4$ we have energies -0.28 , -0.21 per

electron in 0-th and 1-st LL respectively for symmetric state and -0.24 , -0.22 respectively for antisymmetric orbital. Thus we expect symmetric state near 0-th LL and antisymmetric state near the 1-st LL. Calculation shows that one unit-charge ion cannot hold more than 2 electrons in the lowest-energy states: e-e interactions make this too expensive.

Now we consider two positive charges and two electrons. Calculation shows that symmetric orbital state is preferred. The resulting hydrogen-like molecule is very stable with optimal inter-atomic distance $1.2l_B$ and $1.3l_B$ for 1-st and 0-th LL, Fig. 5b.

The same calculation can be repeated for 3 ions bound by two electrons, see Fig.5c. We compare the triangle configuration of ions with a linear chain geometry and find that equilateral triangle geometry has lower energy. Four ions cannot be bound by two electrons. The described equilateral triangle with 2 electrons is prominent for providing the lowest possible energy per electron, thus, it is this configuration that appears first in the phase diagram, Fig. 3.

Considering now 3-electron states in Hartree approximation we found that three electrons cannot form a one-centered wave-function to bind any number of ions since the e-e interaction gets too high and the resulting energy gain can by no means compete with the energy of far-separated smaller clusters described above. Thus, with more electrons, ions will split into stable 1, 2 and 3 ion clusters described above, hence, the classification is complete.

Having studied the possible macro-molecules separately, the results may be combined in a phase diagram. In each of the above states one can find the energy per electron that bind the molecule and thus find a minimal electron chemical potential μ_{\min} for such molecule to appear. For a given electron chemical potential, several molecule configurations may be possible. Let us assume that the number of ions and electron chemical potential are fixed. For a molecule with N ions bound by n electrons we compute the free energy gain per ion by the formula:

$$\Delta E_{\text{ion}} = \frac{(E_{\text{binding}} + E_{\text{Coulomb}}) - \mu n}{N} = \frac{E - \mu N}{N} \quad (9)$$

The configurations with minimal ΔE_{ion} will deliver the minimal free energy at zero temperature, see Fig.

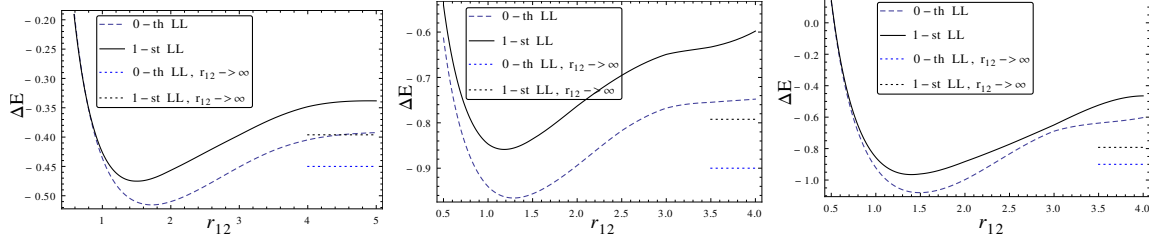


FIG. 5. Energy (electron energy + Coulomb repulsion of ions) of stable macro-molecules. Electron energy is counted from 0 and $\sqrt{2}$ for 0-th and 1-st LLs respectively. Here $\alpha = 0.4$ and $d = 0.05l_B$. Dotted lines mark the $r \rightarrow \infty$ asymptotic to show stability. a) Two ions bound by one electron in graphene; b) Two ions bound by two electrons in symmetric orbital state; c) Three ions forming equilateral triangle bound by two electrons in symmetric state

3. In particular, Fig.3 shows that the state of one electron bound by one ion (lines 4 and 9 on the plot) is never the lowest-energy state. At high chemical potentials (close to the vacuum LL) the state with 2 electrons per one ion wins (lines 5 and 10). All the other states correspond to bound states of 2 or 3 ions, which are realized for $\mu \in [-0.93, -0.08] \cup [0.51, 1.39]$ for the example $\alpha = 0.4$ considered.

Changing α in the leading approximation just linearly scales the phase diagram around the vacuum Landau level (0 and $\sqrt{2}$). As is seen from Fig. 4, the binding of molecules near $\nu = 2$ should additionally increase with increasing α due to noticeable non-linearity.

III. DISCUSSION AND CONCLUSIONS

The above results were obtained for an ideal monolayer graphene sheet at zero temperature. The realistic graphene may have other non-mobile impurities, ripples, corrugations and finite temperature. Clearly, mobile charge impurities can equally well form bound states with non-mobile ones. Simultaneously, charged impurities may introduce smooth inhomogeneities in the chemical potential leading to replacement of chemical potential μ with a local chemical potential $\mu + U_{\text{impurities}}$ in our considerations. It is also important to note that sufficient amount of mobile charged impurities leads to screening of potential landscape thus making it flatter on large scales. This may be one of the keys to understanding of exceptionally precise Hall quantization in epitaxial graphene²⁰.

The temperature and short-range impurities lead to level-broadening. As is clear from Fig. 2, the binding appears when the lowest Landau sub-level is filled, while the next ones are empty. The splitting between these levels is of the order of $\alpha E_B \approx 300\alpha\sqrt{B}/(\text{Tesla})\text{ K}$ (see Fig. 2). The splitting of levels is twice smaller near the 1-st LL, but in this case the second smallest LL is also attractive and population of this level does not spoil the binding. So, with $\alpha \approx 0.4$ our results must survive the room

temperatures and small amount of short-range impurities for magnetic fields above 10 Tesla and even higher temperatures at larger fields. These conclusions are also supported by the experiment of ref. [27]. Note that at room temperature (and even below) many types of ionic impurities are mobile⁴.

Another effect of finite temperature is an entropic contribution coming from the approximate spin and valley degeneracy. This effectively decreases the energy by $k_B T \ln n$, where $n = 4$ for one-electron bound states, $n = 6$ for two-electron symmetric states and $n = 10$ for two-electron anti-symmetric states.

An important aspect in graphene is rippling and corrugations³⁷⁻³⁹. As argued in ref. [40], corrugations in graphene may be described by fluctuations in perpendicular magnetic field that lead to considerable broadening of non-zero LLs. At the same time, the 0-th LL is protected and mainly broadens due to temperature⁴⁰. Our main results correspond to chemical potentials in the gap above or below the 0-th LL, thus the effect of corrugations is expected to be moderate. At the same time, corrugations may kill any weak binding effects that might occur in the higher QHE plateaux.

To summarize, we have shown that graphene in magnetic field can mediate strong attraction of like charges put near graphene. The resulting size and configuration of macro-molecules depend on magnetic length and filling factor and thus can be easily changed by tuning magnetic field or doping of graphene. The results are expected to survive significant temperatures. This opens a thrilling perspective to nanoscopic manipulation of ions on graphene by using macroscopic tools.

Acknowledgements: This work has been supported by EPSRC through grants EP/l02669X/1 and EP/H049797/1. The support of the RSF grant 14-22-00281 is acknowledged. I am indebted to Joseph J. Betouras and Feo V. Kusmartsev for many stimulating discussions and support. Useful correspondence with A.Tzalenchuk, O.Gamayun and G.Berdyyorov is gratefully acknowledged.

* S.Sлизовский@lboro.ac.uk

¹ K. S. Novoselov, A. K. Geim, S. V. Morozov, D. Jiang, M. I. Katsnelson, I. V. Grigorieva, S. V. Dubonos, and A. A. Firsov, *Nature (London)* **438**, 197 (2005), cond-mat/0509330.

² M. Biggs, M. Kiamahalleh, M. Mijajlovic, and M. Penna, *AU2014/900273* (2014).

³ M. Biggs, M. Penna, M. Kiamahalleh, and M. Mijajlovic, *PCT/AU2015/000034* (2015).

⁴ T. O. Wehling, M. I. Katsnelson, and A. I. Lichtenstein, *Phys. Rev. B* **80**, 085428 (2009).

⁵ K.-H. Jin, S.-M. Choi, and S.-H. Jhi, *Phys. Rev. B* **82**, 033414 (2010).

⁶ M. Khantha, N. A. Cordero, L. M. Molina, J. A. Alonso, and L. A. Girifalco, *Phys. Rev. B* **70**, 125422 (2004).

⁷ A. N. Rudenko, F. J. Keil, M. I. Katsnelson, and A. I. Lichtenstein, *Phys. Rev. B* **82**, 035427 (2010), arXiv:1002.2536 [cond-mat.mes-hall].

⁸ P. V. C. Medeiros, A. J. S. Mascarenhas, F. de Brito Mota, and C. M. C. de Castilho, *Nanotechnology* **21**, 485701 (2010).

⁹ S. Y. Davydov and G. I. Sabirova, *Technical Physics Letters* **37**, 515 (2011).

¹⁰ F. Schedin, A. K. Geim, S. V. Morozov, E. W. Hill, P. Blake, M. I. Katsnelson, and K. S. Novoselov, *Nature Materials* **6**, 652 (2007).

¹¹ M. Caragiu and S. Finberg, *Journal of Physics Condensed Matter* **17**, 995 (2005).

¹² A. V. Shytov, D. A. Abanin, and L. S. Levitov, *Phys. Rev. Lett.* **103**, 016806 (2009).

¹³ M. O. Goerbig, *Rev. Mod. Phys.* **83**, 1193 (2011).

¹⁴ S. Slizovskiy and J. J. Betouras, *Phys. Rev. B* **86**, 125440 (2012), arXiv:1203.5044 [cond-mat.mes-hall].

¹⁵ H. Tetlow, J. P. de Boer, I. J. Ford, D. D. Vvedensky, J. Coraux, and L. Kantorovich, *Physics Reports* **542**, 195 (2014).

¹⁶ S. Kim, J. Ihm, H. J. Choi, and Y.-W. Son, *Solid State Communications* **175** **176**, 83 (2013).

¹⁷ Y. Qi, S. H. Rhim, G. F. Sun, M. Weinert, and L. Li, *Phys. Rev. Lett.* **105**, 085502 (2010).

¹⁸ F. Varchon, R. Feng, J. Hass, X. Li, B. N. Nguyen, C. Naud, P. Mallet, J.-Y. Veuillen, C. Berger, E. H. Conrad, and L. Magaud, *Phys. Rev. Lett.* **99**, 126805 (2007).

¹⁹ T. J. B. M. Janssen, A. Tzalenchuk, R. Yakimova, S. Kubatkin, S. Lara-Avila, S. Kopylov, and V. I. Fal'ko, *Phys. Rev. B* **83**, 233402 (2011).

²⁰ A. Tzalenchuk, S. Lara-Avila, A. Kalaboukhov, S. Paolillo, M. Syväjärvi, R. Yakimova, O. Kazakova, T. J. B. M. Janssen, V. Fal'ko, and S. Kubatkin, *Nature Nanotechnology* **5**, 186 (2010), arXiv:0909.1220 [cond-mat.mes-hall].

²¹ J. A. Alexander-Webber, A. M. R. Baker, T. J. B. M. Janssen, A. Tzalenchuk, S. Lara-Avila, S. Kubatkin, R. Yakimova, B. A. Piot, D. K. Maude, and R. J. Nicholas, *Phys. Rev. Lett.* **111**, 096601 (2013).

²² S. Kopylov, A. Tzalenchuk, S. Kubatkin, and V. I. Fal'ko, *Applied Physics Letters* **97**, 112109 (2010), arXiv:1007.4340 [cond-mat.mtrl-sci].

²³ S. Slizovskiy, *Journal of Physics Condensed Matter* **25**, 496007 (2013), arXiv:1305.2527 [cond-mat.mes-hall].

²⁴ M. M. Fogler, D. S. Novikov, and B. I. Shklovskii, *Phys. Rev. B* **76**, 233402 (2007).

²⁵ I. S. Terekhov, A. I. Milstein, V. N. Kotov, and O. P. Sushkov, *Physical Review Letters* **100**, 076803 (2008), arXiv:0708.4263.

²⁶ P. K. Pyatkovskiy and V. P. Gusynin, *Phys. Rev. B* **83**, 075422 (2011), arXiv:1009.5980 [cond-mat.str-el].

²⁷ A. Lucian-Mayer, M. Kharitonov, G. Li, C.-P. Lu, I. Skachko, A.-M. B. Gonçalves, K. Watanabe, T. Taniguchi, and E. Y. Andrei, *Phys. Rev. Lett.* **112**, 036804 (2014).

²⁸ K. S. Novoselov, Z. Jiang, Y. Zhang, S. V. Morozov, H. L. Stormer, U. Zeitler, J. C. Maan, G. S. Boebinger, P. Kim, and A. K. Geim, *Science* **315**, 1379 (2007).

²⁹ Y. Zhang, Y.-W. Tan, H. L. Stormer, and P. Kim, *Nature (London)* **438**, 201 (2005), cond-mat/0509355.

³⁰ V. P. Gusynin and S. G. Sharapov, *Phys. Rev. Lett.* **95**, 146801 (2005).

³¹ N. M. R. Peres, F. Guinea, and A. H. Castro Neto, *Phys. Rev. B* **73**, 125411 (2006).

³² O. V. Gamayun, E. V. Gorbar, and V. P. Gusynin, *Phys. Rev. B* **83**, 235104 (2011).

³³ Y. Zhang, Y. Barlas, and K. Yang, *Phys. Rev. B* **85**, 165423 (2012).

³⁴ This way we may consider a hole in the “dead layer” of SiC epitaxial graphene as a mobile impurity.

³⁵ This will not be the case for the ordinary 2D electron gas since the quasiparticle mass will essentially enter the game.

³⁶ A. H. Castro Neto, F. Guinea, N. M. R. Peres, K. S. Novoselov, and A. K. Geim, *Reviews of Modern Physics* **81**, 109 (2009), arXiv:0709.1163.

³⁷ S. V. Morozov, K. S. Novoselov, M. I. Katsnelson, F. Schedin, L. A. Ponomarenko, D. Jiang, and A. K. Geim, *Phys. Rev. Lett.* **97**, 016801 (2006).

³⁸ J. C. Meyer, A. K. Geim, M. I. Katsnelson, K. S. Novoselov, T. J. Booth, and S. Roth, *Nature (London)* **446**, 60 (2007), cond-mat/0701379.

³⁹ M. I. Katsnelson and K. S. Novoselov, *Solid State Communications* **143**, 3 (2007), cond-mat/0703374.

⁴⁰ A. J. M. Giesbers, U. Zeitler, M. I. Katsnelson, L. A. Ponomarenko, T. M. Mohiuddin, and J. C. Maan, *Phys. Rev. Lett.* **99**, 206803 (2007).